THE SPRING RESEARCH AND MANUFACTURERS' ASSOCIATION

THE APPLICATION OF THE THEORY OF FRACTURE MECHANICS TO THE FAILURE BEHAVIOUR OF SPRINGS AND SPRING MATERIALS

by

P. F. Timmins, M.Sc., A.Met.,

M.I.M., M. Inst.P.

Report No. 254

May 1976

THE SPRING RESEARCH AND MANUFACTURERS' ASSOCIATION

Report No. 254

THE APPLICATION OF THE THEORY OF FRACTURE MECHANICS TO THE FAILURE BEHAVIOUR OF SPRINGS AND SPRING MATERIALS

SUMMARY

The concepts of linear elastic and post-yield fracture mechanics are described using the stress intensity approach. Failure under conditions of static and cyclic loading is considered and a single test piece design is reported to be suitable for testing in both loading conditions. The principal aim is to use the concepts of fracture mechanics to relate service conditions applicable to leaf and helical springs to laboratory testing.

The suggestion is made that future work should involve stress corrosion testing using the stress intensity approach.

May 1976

CONTENTS

CONTENTS (Cont.)

Report No. 254

THE APPLICATION OF THE THEORY OF FRACTURE MECHANICS TO THE FAILURE BEHAVIOUR OF SPRINGS AND SPRING MATERIALS

by

P. F. Timmins, M.Sc., A.Met., M.I.M., M.Inst.P.

1. INTRODUCTION

The aims of fracture mechanics, now widely employed in industry, are to relate laboratory tests realistically to actual service conditions and to provide a quantitative relationship between the applied stress, the size of a stress concentrator, such as a small rolling crack, and the material toughness.

Less informative tests are still used, however; notched-bar impact testing data, for example, which have been utilised over the years for spring materials, do not provide a quantitative measure of material toughness, because the measurements made cannot be converted into a form that can be used directly by design engineers. Neither the transition temperature nor the amount of energy absorbed at a given temperature can be reconciled easily with the designer's parameters of stress and dimensions.

The fracture mechanics or "stress intensity" approach to the failure behaviour of spring materials, in terms of crack propagation or growth rates, may be applied in conditions of cyclic loading. The advantage of this approach over conventional S/N curves is that a measure can be made of the influence of changing stress intensity at a fatigue crack tip on the rate at which the crack grows or propagates.

2. THE FRACTURE MECHANICS OF TENSILE LOADED PRE-CRACKED PLATES

When a pre-existing crack in a brittle plate subject to an applied tensile load grows by increasing its area by a small amount δA, a small amount of energy δQ is absorbed in the process and the stored strain energy of the specimen is decreased by a small amount δV. When the condition:

$$-\frac{\delta V}{\delta A} = \frac{\delta Q}{\delta A}$$

is attained, it is possible for the crack to grow without the need for additional work to be done by the applied load and the crack propagates rapidly. Griffith[1] associated the energy absorbed δQ with the surface energy of the growing crack, 2γ, where γ is the surface energy of the solid, thus obtaining the relationship for an infinitely long, thin plate (i.e. plane stress):

$$\sigma_F = \left(\frac{2E\gamma}{\pi a}\right)^{\frac{1}{2}} \quad \ldots\ldots\ldots 1$$

where σ_F is the fracture stress, E is Young's modulus and 2a the crack length.

For an infinitely long plate, which is thick compared to the length of the crack (plane strain), the equation is:

$$\sigma_F = \left[\frac{2E\gamma}{(1-\nu^2)\pi a}\right]^{\frac{1}{2}} \quad \ldots\ldots\ldots 2$$

where ν is Poisson's ratio.

2.1 Modification of Griffith's Theory

The Griffith theory was developed for glass and does not apply to metals. Orowan[2] pointed out that energy, usually far in excess of γ, is absorbed by plastic deformation in the vicinity of the propagating crack. It is necessary, therefore, to modify relationships 1 and 2 to include a term to take account of the plastic deformation due to the stress distribution around the crack tip, γ_p,

i.e:

$$\sigma_F = \left[\frac{2E(\gamma + \gamma_p)}{\pi a}\right]^{\frac{1}{2}} \quad \ldots\ldots\ldots\ldots 3$$

where $\gamma + \gamma_p$ is the fracture energy.

Similarly, in plane strain:

$$\sigma_F = \left[\frac{2E(\gamma + \gamma_p)}{(1 - \nu^2)\pi a}\right]^{\frac{1}{2}} \quad \ldots\ldots\ldots\ldots 4$$

Since $\gamma_p >> 2\gamma$, the surface energy term may be neglected, thus:

$$\sigma_F = \left(\frac{2E\gamma_p}{\pi a}\right)^{\frac{1}{2}} \quad \ldots\ldots\ldots\ldots 5$$

In terms of the strain energy release rate, G, due to Irwin[3] the critical value of G is given by $G_{crit} = 2\gamma_p$, so that:

$$\sigma_F = \left(\frac{EG_{crit}}{\pi a}\right)^{\frac{1}{2}} \quad \ldots\ldots\ldots\ldots 6$$

Similarly:

$$K_{crit} = \sigma_F\sqrt{\pi a} = \sqrt{EG_{crit}} \quad \ldots\ldots\ldots\ldots 7$$

where K_{crit} is a critical value of the stress intensity at the crack tip.

In plane strain:

$$\sigma_F = \left[\frac{EG_{crit}}{(1 - \nu^2)\pi a}\right]^{\frac{1}{2}} \quad \ldots\ldots\ldots\ldots 8$$

and:

$$K_{crit} = \left[\frac{EG_{crit}}{(1 - \nu^2)}\right]^{\frac{1}{2}} \quad \ldots\ldots\ldots\ldots 9$$

G_{crit} is commonly referred to as the fracture toughness[3] and the above <u>idealised</u> expressions provide the basis for the study of this phenomenon in materials.

In recent years, however, less emphasis has been given to the energy release rate approach to fracture; it is now more usual to express fracture toughness in terms of K rather than G values. There are several reasons for this. Firstly, K varies linearly with the applied load or nominal stress for a fixed specimen shape. Secondly, it is more logical to consider stress-strain distribution at crack tips, rather than energy balances, as determining the conditions for fracture. Moreover, K values can be determined directly from laboratory tests, while G values must be calculated from relationship 7.

2.2 Modes of Crack Opening

Irwin[3] developed a notation for the opening modes, which is now widely used. The various modes are illustrated in Fig. 1. Mode I, the tensile mode, is applicable to the formulae considered in the previous section. Mode II cracking is characterised by shear displacements at right angles to the crack front. Mode III, the antiplane strain mode, involves shear displacement parallel to the crack front. Thus the terms, K_I, K_{II} and K_{III} and their counterparts G_I, G_{II} and G_{III} define the stress intensity (K) or the strain energy release rate (G) for particular modes of crack opening, as denoted by the Roman subscripts. The K or G value for catastrophic failure, i.e. fast fracture, is denoted by the subscript C. K_{IC} or G_{IC} values are usually quoted for the plane strain case, K_C or G_C without a Roman subscript denoting plane stress fracture toughness.

2.3 Plastic Deformation at Crack Tips- The Plastic Zone Size

A crack in most solids cannot grow without plastic deformation taking place at the crack tip. The size of this zone of plastic deformation is a function of the macroscopic yield stress, σ_y, (usually taken as the value of 0.2% proof stress) of the material and the stress intensity, K. If r_p is the plastic zone radius, then in plane stress:[4]

$$r_p = \frac{1}{2\pi}\left(\frac{K}{\sigma_y}\right)^2 \quad \ldots\ldots\ldots 10$$

and in plane strain:

$$r_p = \frac{1}{6\pi}\left(\frac{K_I}{\sigma_y}\right)^2 \quad \ldots\ldots\ldots 11$$

However, there is no precise change over point from plane stress to plane strain, but as a general guide, when the specimen thickness B and the crack length a $\geq 2.5\left(\frac{K_I}{\sigma_y}\right)^2$, then plane strain prevails. Conversely, when B and a $<< 2.5\left(\frac{K_I}{\sigma_y}\right)^2$, plane stress is the principal mode. However, when the size of the plastic zone is such that the net section stress exceeds 0.8 σ_y, linear elastic fracture mechanics no longer provides an adequate description of the stress field at the crack tip and the concept of post-general yield fracture mechanics is dominant. Important in this concept is the Crack Opening Displacement, C.O.D.[5]

2.4 C.O.D.

The physical principle underlying the use of C.O.D. is that, to extend a crack, the material just ahead of the crack tip must be strained sufficiently to be parted by whichever fracture mechanism (not mode) is operative. In plane stress, for all stresses below the general yield stress, σ_y, the C.O.D., δ is given by[6]:

$$\delta = \frac{8\delta_y}{\pi E} a \ln \sec\left(\frac{\pi\sigma_{app}}{2\sigma_y}\right) \quad \ldots\ldots\ldots 12$$

where σ_{app} is the applied stress.

For "brittle" fractures, equation 12 becomes:

$$\sigma_F = \sigma_{app} = \left(\frac{E\sigma_y \delta_{crit}}{\pi a}\right)^{\frac{1}{2}} \quad \ldots\ldots\ldots 13$$

where δ_{crit} is the critical C.O.D. Or, in simpler terms:

$$G_{crit} = \sigma_y \delta_{crit} = f(K) \quad \ldots\ldots\ldots\ 14$$

C.O.D. may therefore be related to K, as is shown in Fig. 2 for example. By examining fracture surface of C.O.D. specimens the degreee of quasi-microplastic deformation at the crack tip preceding failure may be related to C.O.D. This is the so-called "stretch-zone width" - C.O.D. relationship[7], as shown in Fig. 3. It is therefore possible to determine the fracture toughness of a material from the inter-relationship of these parameters.

3. FATIGUE AND FRACTURE MECHANICS

Some of the typical terms associated with fatigue are shown in Fig. 4.

Fatigue tests are conducted using a stress of load cycle similar to that shown in Fig. 4. This traditional test is carried out until failure occurs and the data obtained are plotted on a stress/number-of-cycles-to-failure curve, referred to as an S-N curve, as shown in Fig. 5.

It is evident from Fig. 5 that S-N curves show only one stage in the fatigue process, i.e. the number of cycles at which failure occurs. The stage at which crack nucleation takes place and the growth of a crack preceding final fracture are not shown. The fatigue process can be divided into stages of cycles to initiation (or nucleation) and cycles to failure, with a growth or propagation stage in between, as depicted in Fig. 6.

Obviously, to utilise materials efficiently it would be desirable to avoid dealing with propagation, i.e. growth, and final fracture. However, because of performance requirements, this is not always feasible. Thus, a means

of dealing with fatigue crack propagation must be devised. This is normally accomplished by conducting fatigue tests on panels or components that contain some kind of pre-existing flaw, such as a crack or a notch. As the load cycles are applied, the crack grows. During the test the growth of the crack is monitored and recorded with the number of cycles to produce a crack of known size. This information is plotted on a curve of the type shown in Fig. 7.

These data can then be differentiated to determine the crack growth rate per cycle, $\frac{da}{dN}$. The crack growth rate can then be plotted versus the change in stress intensity (because the crack is extending), ΔK.

For many materials, subjected to a wholly tensile loading cycle, the rate of crack growth can be expressed by an equation of the type:

$$\frac{da}{dN} = C\,(\Delta K)^m \qquad \ldots\ldots\ldots\ldots \quad 15$$

where C is a material constant and m is an exponent, usually about 3. There are at least thirty-three relationships of this type in the literature[8].

4. REAL SPECIMENS, REAL TESTS AND MEANINGFUL DATA

The determination of K in real specimens is more complex than equation 7 implies. The restriction imposed on a crack in a specimen due to the boundaries of the specimen must be considered.

For the CKS tension specimen shown in Fig. 8[9]:

$$K_I = \frac{PY_2}{BW^{\frac{1}{2}}} \qquad \ldots\ldots\ldots\ldots \quad 16$$

where the compliance, Y_2, is given by:

$$Y_2 = \left[29.6\left(\frac{a}{w}\right)^{1/2} - 185.5\left(\frac{a}{w}\right)^{3/2} + 655.7\left(\frac{a}{w}\right)^{5/2} - 1017\left(\frac{a}{w}\right)^{7/2} + 638.9\left(\frac{a}{w}\right)^{9/2}\right] \quad \ldots\ldots \quad 17$$

Y_2 is sometimes referred to as the "stress intensity coefficient". Similarly, if the same specimen is used as a fatigue specimen, K_I in equation 16 is replaced by ΔK, calculated from:

$$\Delta K = K_{max} - K_{min} \quad \ldots\ldots\ldots\ldots \quad 18$$

However, since fatigue is a growth process, K at the crack tip may increase as the crack length increases. To overcome this problem the "constant K" specimen was designed[4], as shown in Fig. 9.

K is derived from the relationship:

$$\frac{K_I \, BW^{1/2}}{P} = 10.9$$

$$\left(0.2 \leq \frac{a}{w} \leq 0.5\right) \quad \ldots\ldots\ldots\ldots \quad 19$$

for which $\Delta K = K_{max} - K_{min}$.

It has recently been pointed out[4], however, that in fatigue, steady state conditions, pertaining to the instantaneous value of ΔK, are always maintained at the crack tip. In other words, the original CKS specimen may be used.

Crack extension is frequently monitored by the Potential Drop Monitoring Technique[10]. Here a constant d.c. current is passed through the specimen and the change in resistance of the specimen as the crack grows is detected by measuring the change in potential across the open mouth of the starter crack (or notch). Optimum positions for the attachment of current leads and potential measuring probes are shown in Fig. 10 for 'uniform current' configurations in a CKS test piece[11].

Calibration curves are determined for a given specimen configuration by plotting:

$\frac{V}{V_o}$ versus $\frac{a}{w}$, e.g. Fig. 14, where $\frac{V}{V_o}$ refers to the potential drop V, across the notch at any crack length ratio, $\frac{a}{w}$, divided by the potential drop V_o, corresponding to an initial crack length ratio of $f(\frac{a}{w})$.

For static tests, a clip gauge, as shown in Fig. 19, is often fixed to the notch gap, so that the C.O.D. can be obtained from[6,10]:

$$\frac{V_c}{\delta_c} = \frac{a + Z}{r(W-a)} + 1 \qquad \ldots\ldots\ldots\ldots 20$$

where V_c = clip gauge displacement
c = crack tip C.O.D.
a = total crack length
W = test piece width
Z = distance of clip gauge from test piece surface
r = rotational factor $= \frac{1}{3}$

For fatigue tests a subtle method of determining $\frac{da}{dN}$ is a fractographic technique which required the use of a scanning electron microscope[8]. Measurements of fatigue striations can be made on a fractograph, as shown in Fig. 11, or whilst the fractured specimen is in the scanning electron microscope. Assuming one striation corresponds to one cycle:

$$\frac{da}{dN} = \frac{1}{\text{magnification}} \times \frac{\text{distance on fractograph}}{\text{striation count/unit distance on fractograph}} \qquad \ldots\ldots\ldots 21$$

Several types of curve are thus produced. For fatigue failure, a $\frac{da}{dN}$ versus ΔK curve may be produced, as shown in Figs. 13 - 16.

5. DISCUSSION

The use of the CKS specimen without modification is satisfactory when leaf springs are being considered, since K_I conditions apply in static and cyclic loading conditions. When considering helical torsion springs and torsion bars, however, the state of stress in the spring must be understood in order to relate in-service stress states to conditions of loading in laboratory test-pieces. The state of stress in a loaded helical spring or a torsion bar is shown in Fig. 17.

Under these conditions, i.e. in a perfectly elastic, isotropic, homogeneous solid, $\sigma_1 = T_{max} = -\sigma_3$. However, in practice, the majority of failures observed in helical springs occur in the tensile mode i.e. $\sigma_1 > T_{max} = -\sigma_3$. The reason proposed for this behaviour is that part of the hydrostatic component, $-\sigma_3$, in a real metal is added to the tensile component due to work hardening at the crack tip[12], such that the gross resolved tensile stress is σ_1 + (a component of $-\sigma_3$), i.e. the situation is akin to carrying out a tensile test under superposed hydrostatic pressure[12]. Since the hydrostatic component does not affect shear processes[12] T_{max} will remain the same. Irrespective of the opening mode, be it K_I, K_{II} or K_{III}, the propagation mode in tension, therefore, is always K_I. Accordingly, the K_I opening CKS specimen may be used to relate behaviour in laboratory tests to the in-service behaviour of both helical and leaf springs, in static and cyclic loading conditions. The starter notch in the CKS specimen must be sharpened by a fatigue crack prior to testing, since fracture toughness has been shown to vary with root radius (see Fig. 18); care must be taken to grow these cracks at low cyclic stresses, so that the effect of fatigue damage on the material properties at the crack tip is minimised[4].

The results obtainable from static and cyclic loaded CKS specimens yield two sets of data. From the static test,

values of K_{IC}, K_I, C.O.D. and stretch-zone width may be obtained by the methods outlined. Similarly, in cyclic loading, $\frac{da}{dN}$ may be obtained by one of the methods described and a value of ΔK_{IC} may be obtained from Region C in Fig. 12. From the relationship shown in Fig. 12, the nucleation stage may also be derived, together with the steady state growth stage and, for a given material, a relationship of the type described by equation 15 may be obtained.

6. CONCLUSIONS

1. The fracture mechanics approach to the fracture behaviour of spring materials allows the nucleation, growth or propagation stages of fracture to be obtained. The rate of crack growth and the fatigue fracture toughness may also be derived.

2. In static tests, the material fracture toughness and the crack-opening displacement may also be obtained.

3. The static and cyclic loading data may be obtained using the CKS type specimen.

7. FUTURE WORK

Initial testing should be confined to the more commonly employed materials such as En 45 and Cr-V steels. The behaviour of materials in corrosive environments should be studied and values for K_{Iscc} (K_I stress-corrosion-cracking) obtained. A comparison may then be drawn between the plane strain toughness of materials in air, K_I, and the plane strain toughness in aggressive environments, K_{Iscc}.

8. ACKNOWLEDGEMENT

The author is indebted to Dr. A. S. Wronski, Reader in Materials Science, University of Bradford, for his useful comments on the manuscript.

9. REFERENCES

1. GRIFFITH A. A. "The Phenomena of Rupture and Flow in Solids". Proc. Roy. Soc., Series A, 221, 1920.

2. OROWAN E. "Fracture and Strength of Solids; Report on Progress in Physics". Phys. Soc., London, 1949.

3. IRWIN G. R. "Fracture Dynamics, Fracturing of Metals". A.S.M., 1948.

4. KNOTT J. F. "Fundamentals of Fracture Mechanics". Butterworths, 1973.

5. British Standard Draft for Development 19:1972.

6. DUGDALE D. S. AND RUTZ C. "Elasticity for Engineers". McGraw-Hill, 1971.

7. HARRIS D. "The Practical Significance of Stretch Zones in Fracture Toughness Testing". Conf. Mech. and Phy. of Fracture, Paper 12, Churchill College, 1975.

8. HOEPPNER D. W. AND KRUPP W. E. "Prediction of Component Life by Application of Fatigue Crack Growth Knowledge". Eng. Frac. Mech., 6, 1974, pp. 47 - 70.

9. British Standard Draft for Development 3:1971.

10. McINTYRE P. "Advanced Methods for Monitoring Fatigue Crack Growth". J. Soc. Env. Eng., September 1974, pp. 3 - 7.

11. RITCHIE R. Ph.D. Thesis, University of Cambridge, 1973.

12. TIMMINS P. F. AND WRONSKI A. S. "Cleavage Fractures of an Fe-Co-V Alloy under Superposed Hydrostatic Pressure". High Temperatures - High Pressures, In the Press.

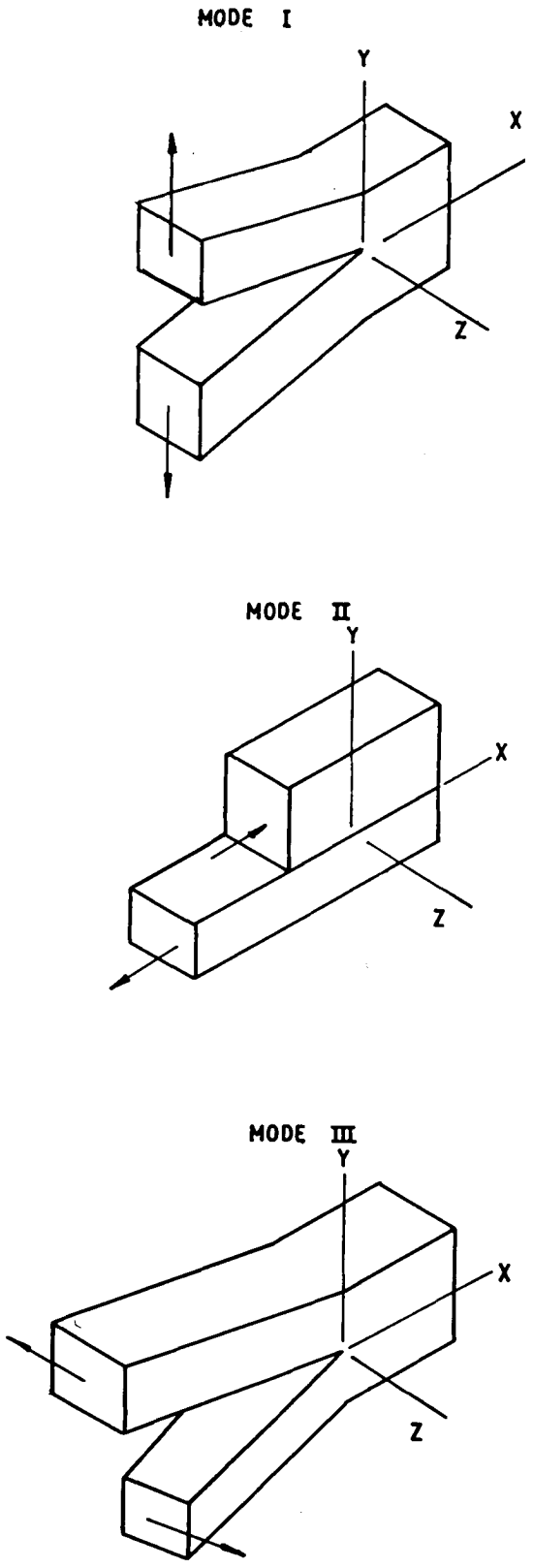

FIG. 1 BASIC MODES OF CRACK SURFACE DISPLACEMENTS. (AFTER IRWIN)

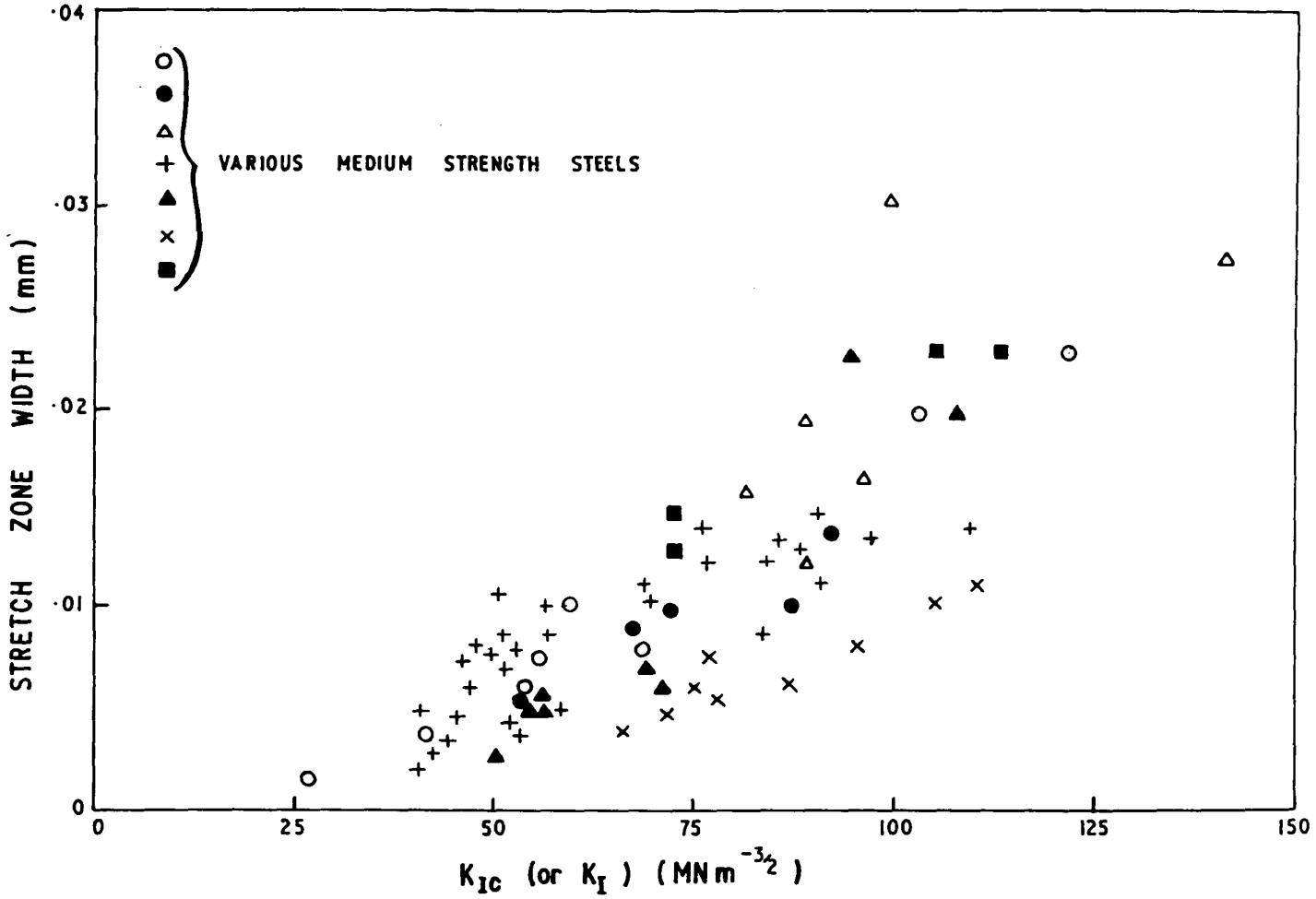

FIG. 2 DEPENDENCE OF STRETCH ZONE WIDTH ON FRACTURE TOUGHNESS K_{IC} (OR K_I) (FROM REF. 6)

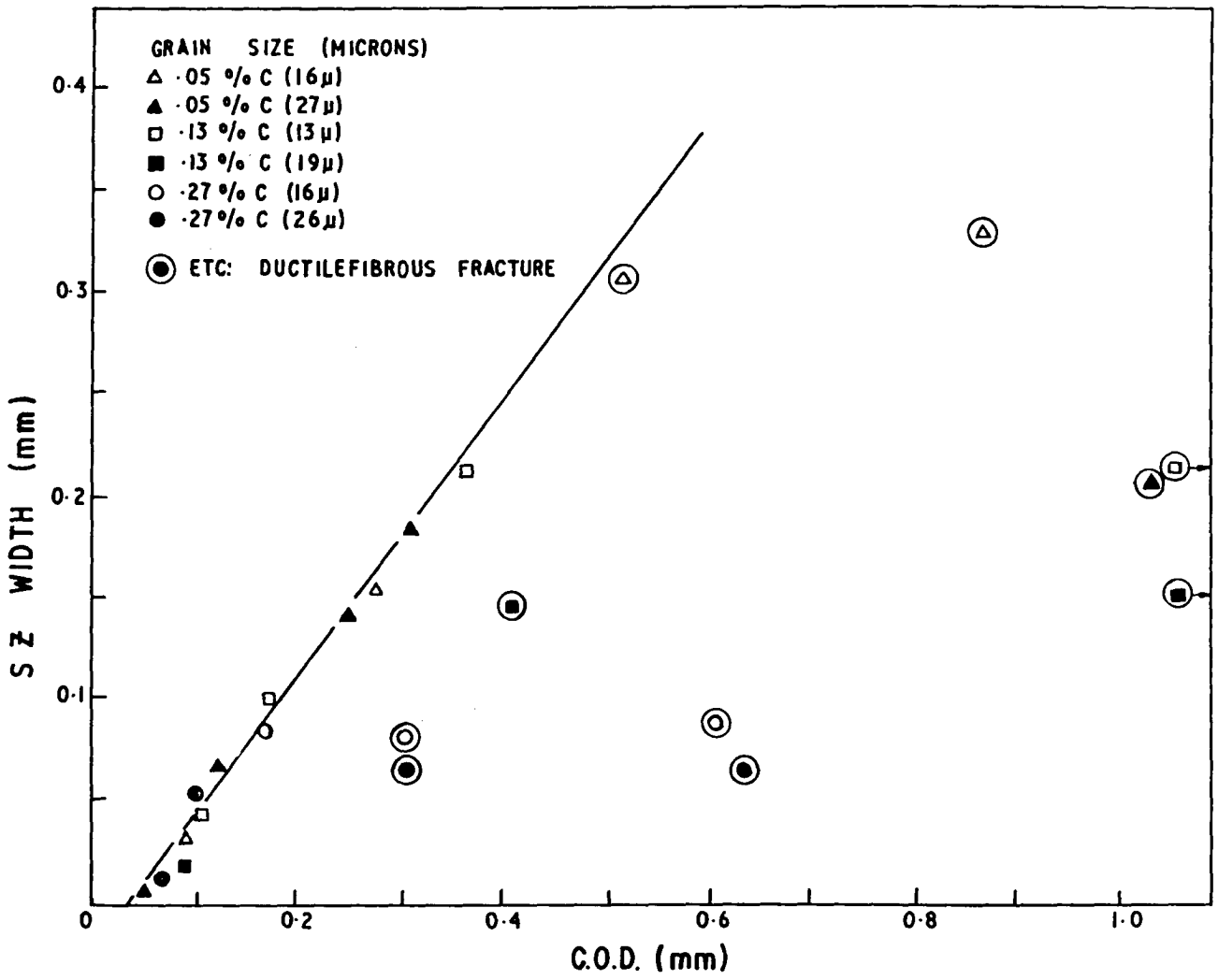

FIG. 3 COMPARISON OF STRETCH ZONE WIDTH MEASUREMENTS AND COD FOR VARIOUS C-Mn STEELS WITH DIFFERENT GRAIN SIZES AND CARBON CONTENTS (FROM REF. 6)

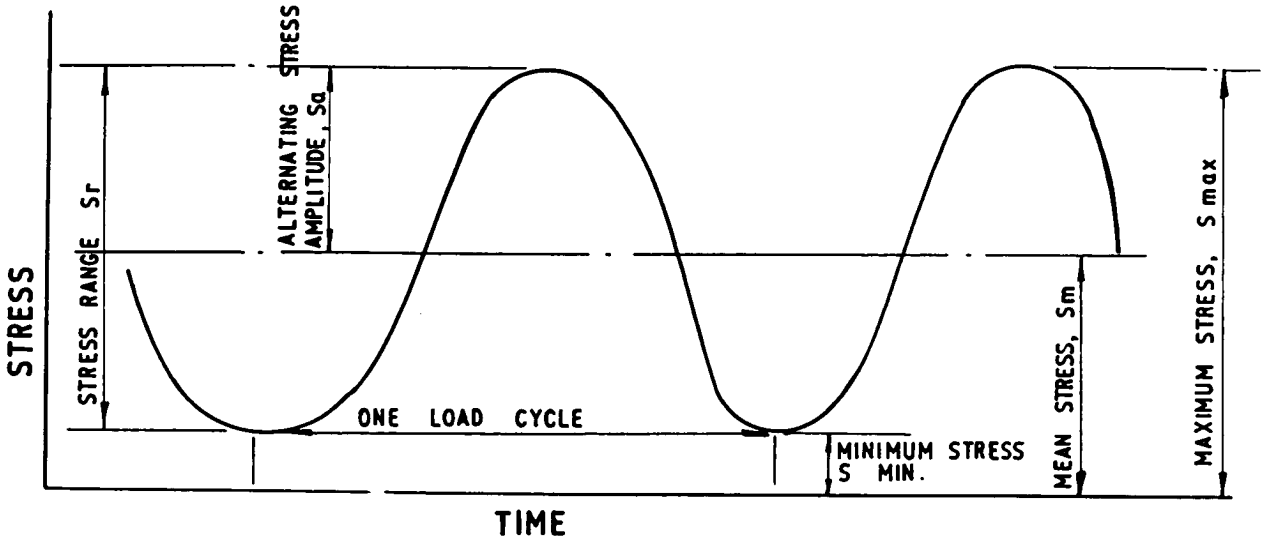

NOTE :- $S_m = \frac{S\,max + S\,min}{2}$, $Sr = S\,max - S\,min$

$Sa = \frac{Sr}{2} = \frac{S\,max - S\,min}{2}$

R or A = STRESS RATIO

$R = \frac{S\,min}{S\,max}$ $A = \frac{Sa}{Sm}$

$R = \frac{1-A}{1+A}$ $A = \frac{1-R}{1+R}$

FIG. 4 NOMENCLATURE USED IN FATIGUE.

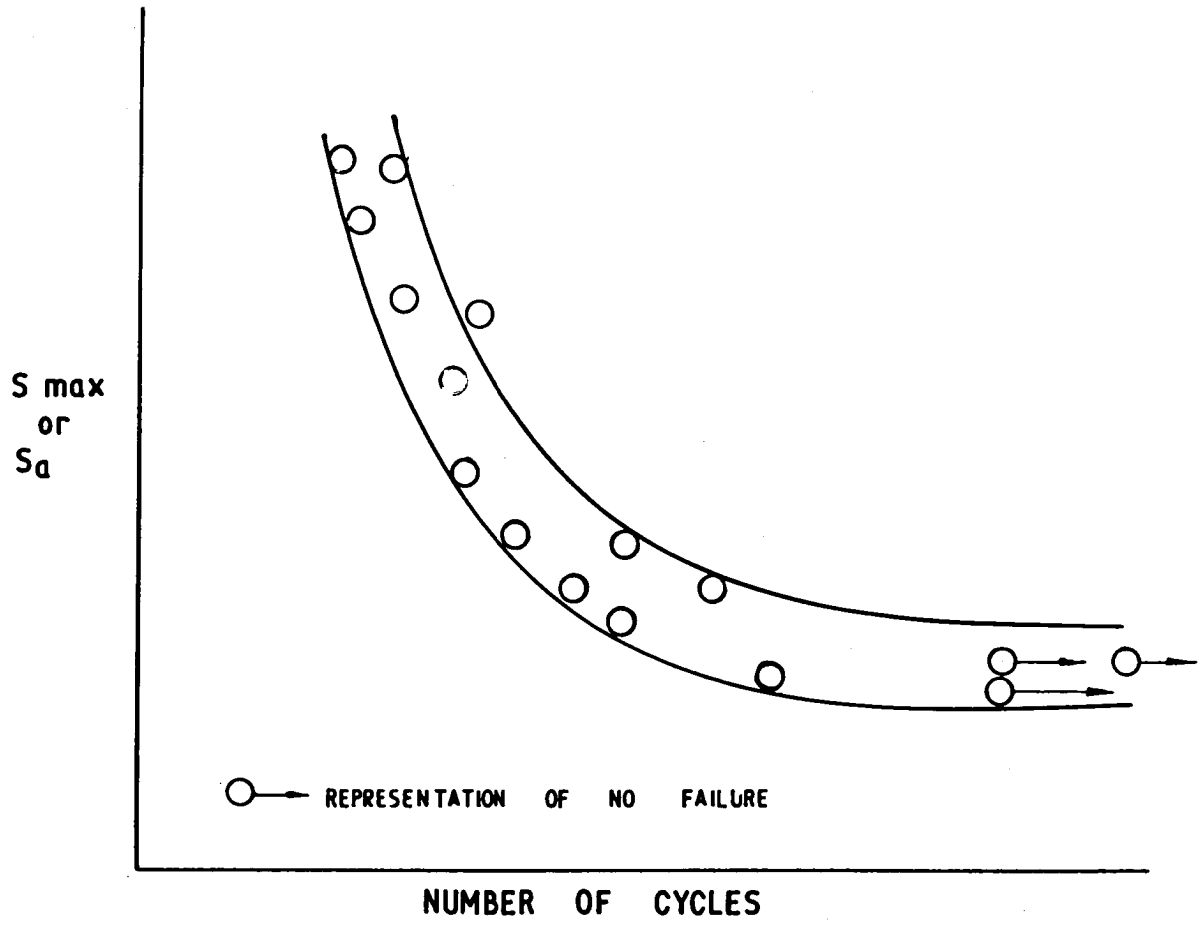

FIG. 5 TYPICAL STRESS/ CYCLES TO FAILURE (S-N) DIAGRAM

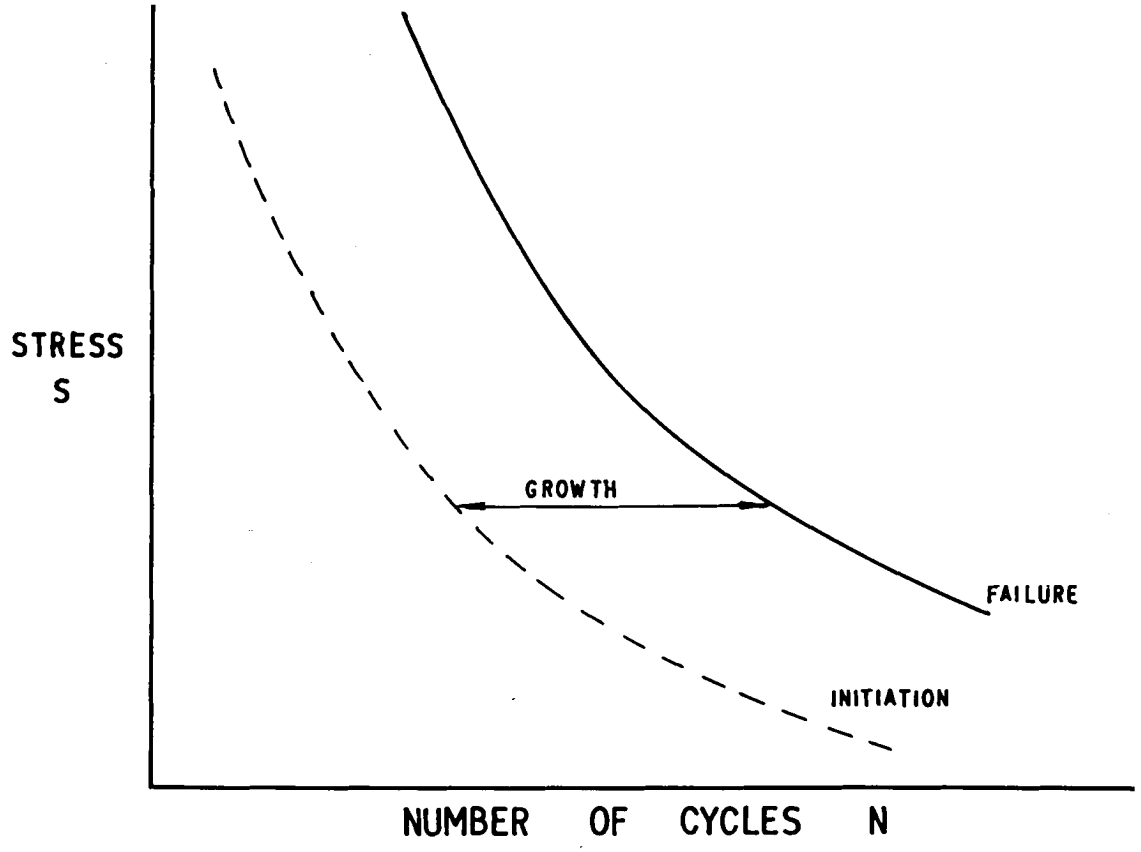

FIG. 6 FATIGUE PROCESS – CYCLES TO INITIATION, CYCLES TO FAILURE.

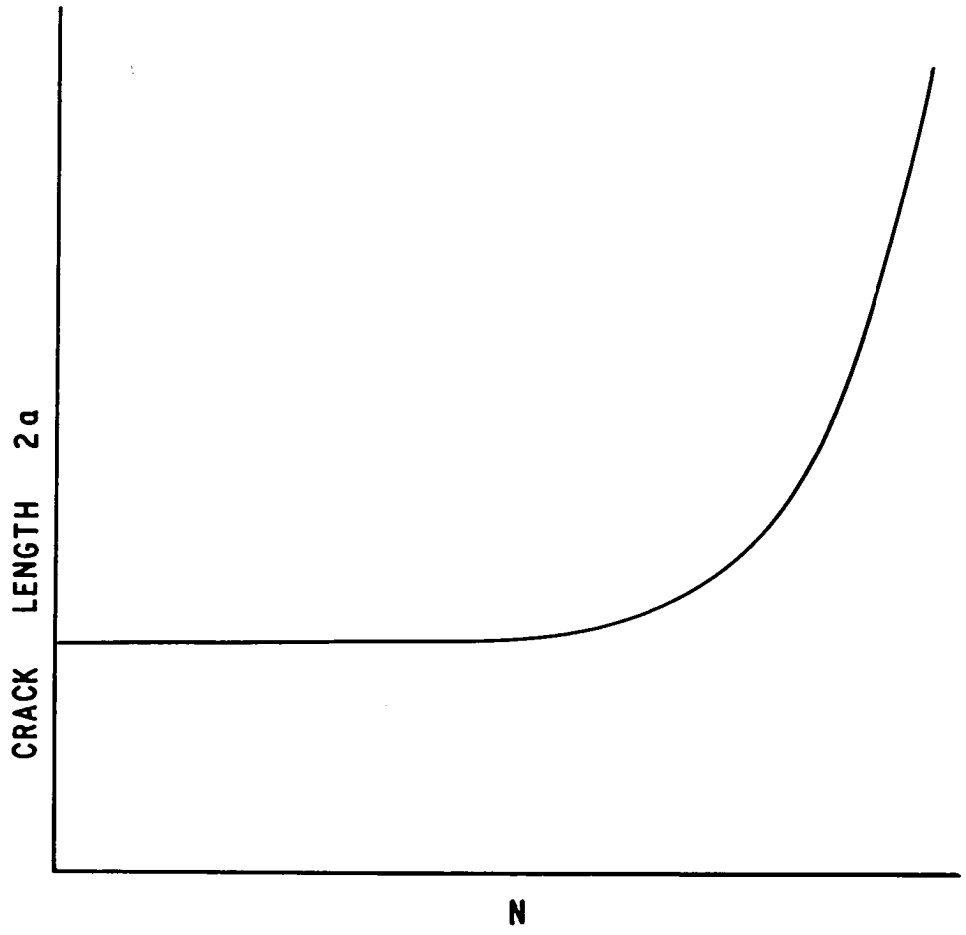

FIG. 7 CRACK GROWTH OR PROPAGATION BEHAVIOR.

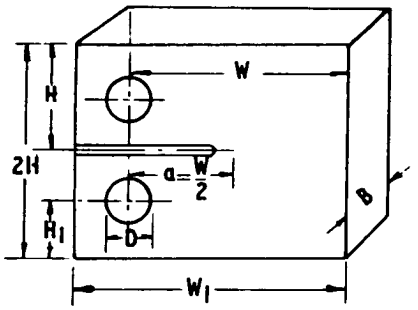

W = 2·0B D = 0·5B
a = 1·0B W_1 = 2·5B
H = 1·2B H_1 = 0·65 B

TYPE	ESTIMATED MEASURED CAPACITY * K_{1c}/σ_{ys}	$(K_{1c}/\sigma_{ys})^2$	TENTATIVE OVERALL DIMENSIONS Thickness (in)	Height (in)	Width (in)
1T-CT	0·63	0·40	1	2·4	2·5
2T-CT	0·90	0·80	2	4·8	5·0
3T-CT	1·10	1·20	3	7·2	7·5
4T-CT	1·30	1·60	4	9·6	10·0
6T-CT	1·60	2·40	6	14·4	15·0
8T-CT	1·80	3·20	8	19·2	20·0
10T-CT	2·00	4·00	10	24·0	25·0
12T-CT	2·20	4·80	12	28·8	30·0

* BASED ON CURRENTLY SUGGESTED ASTM E-24 MINIMUM SIZE CRITERION, a AND B $\geq$ 2·5 $(K_{1c}/\sigma_{ys})^2$

FIG. 8 RECOMMENDED DESIGN FOR COMPACT TENSION TOUGHNESS SPECIMEN. (FROM REF. 4)

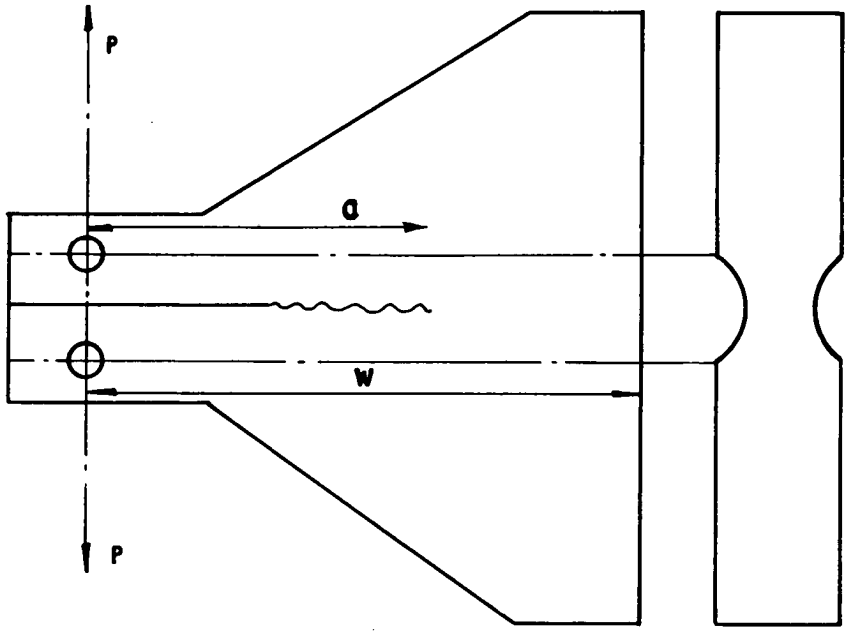

FIG. 9 CONSTANT K SPECIMEN (FROM REF. 4)

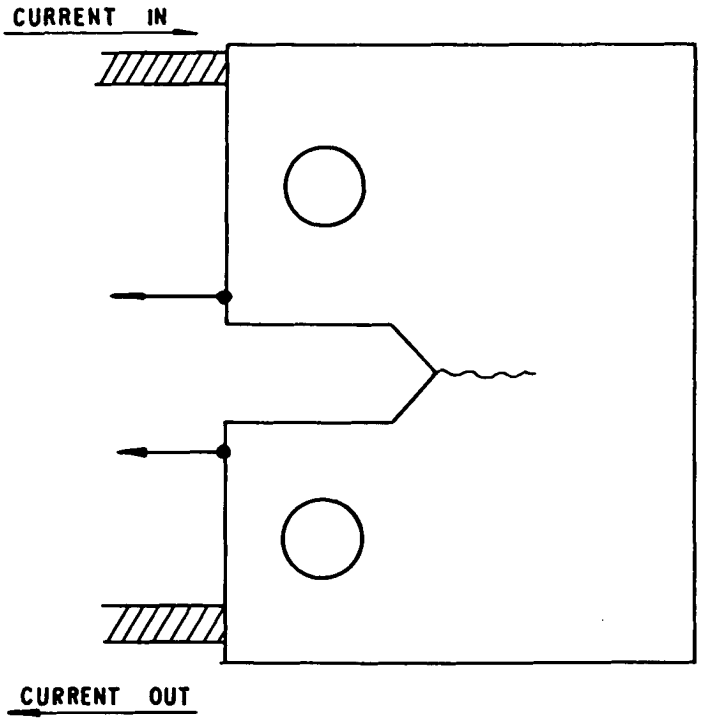

FIG. 10 OPTIMUM POSITIONS FOR CURRENT LEADS AND MEASUREMENT PROBES ON A CKS TEST PIECE. (FROM REF. 9)

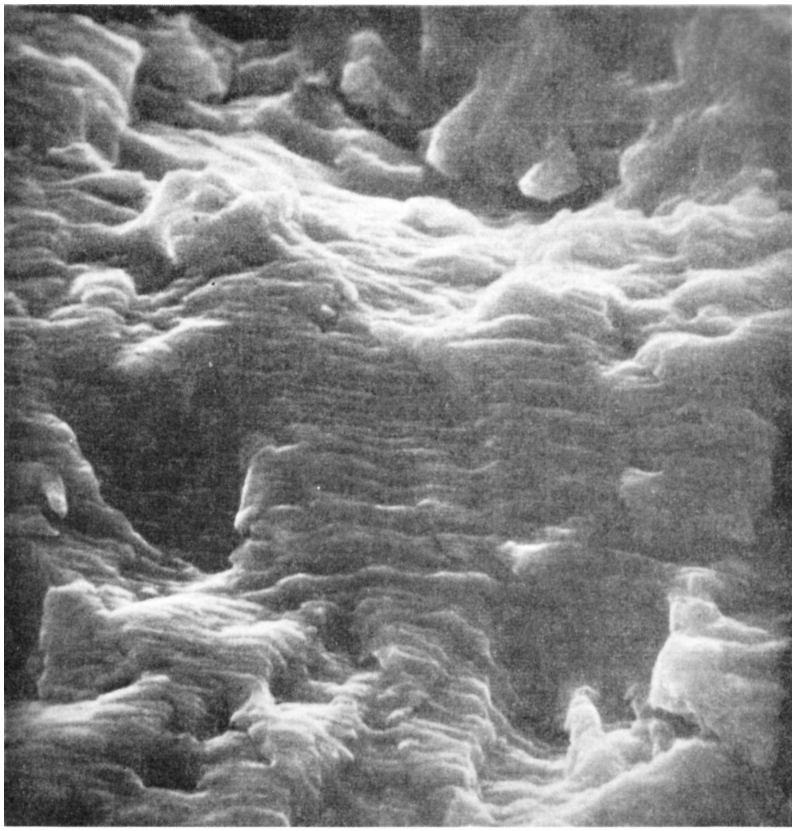

FIG. 11 FATIGUE STRIATIONS ON A SPECIMEN OF SWEDISH IRON, (SCANNING ELECTRON MICROGRAPH).

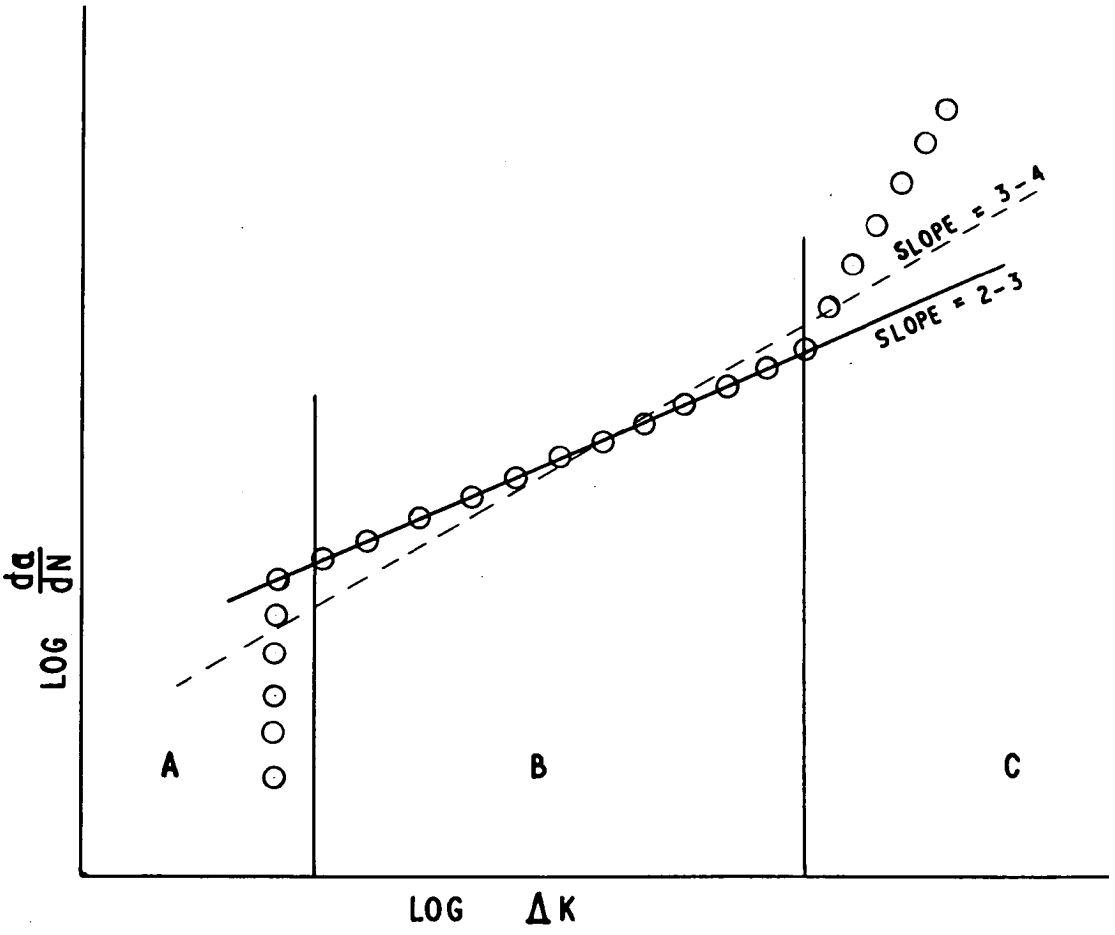

FIG. 12. SCHEMATIC GROWTH RATE DEPENDENCE ON K.
(FROM REF. 4)

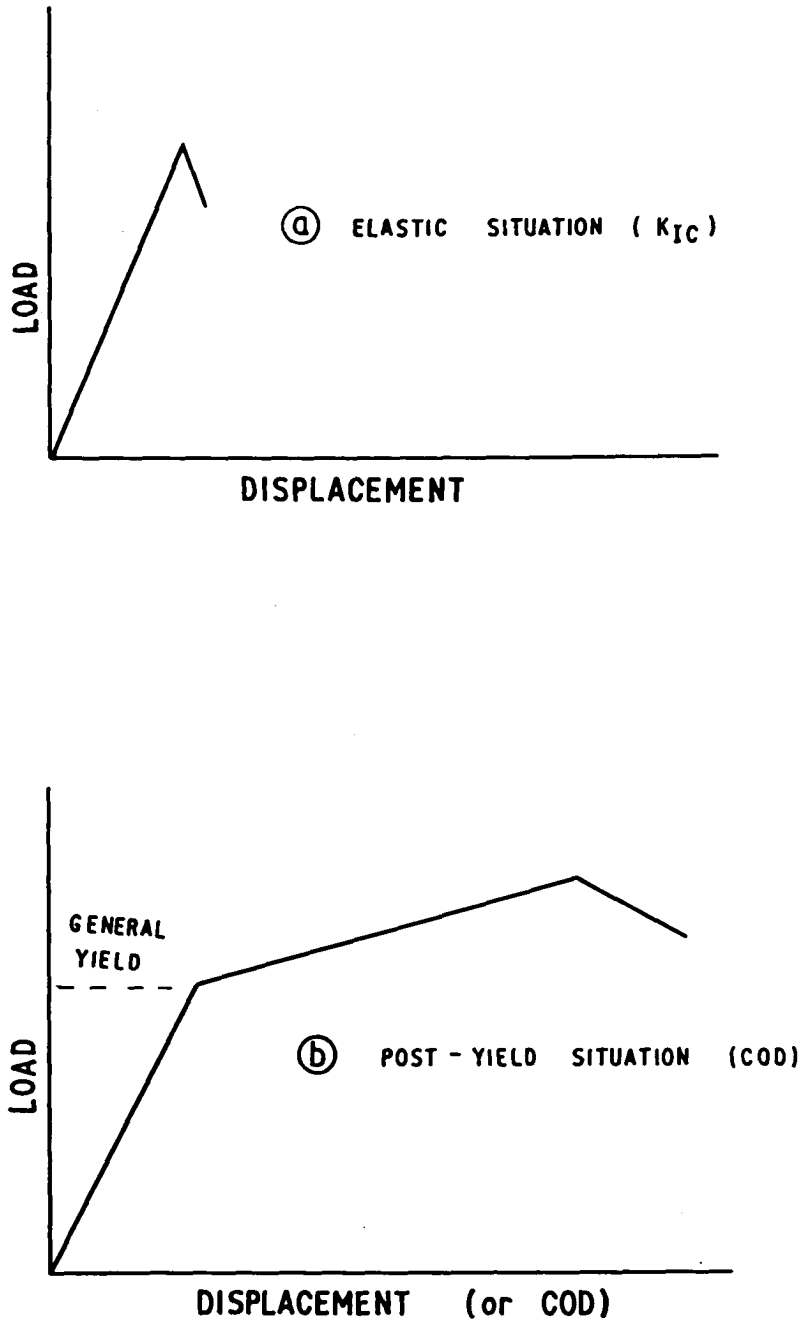

FIG. 13. LOAD/ DISPLACEMENT CURVES.

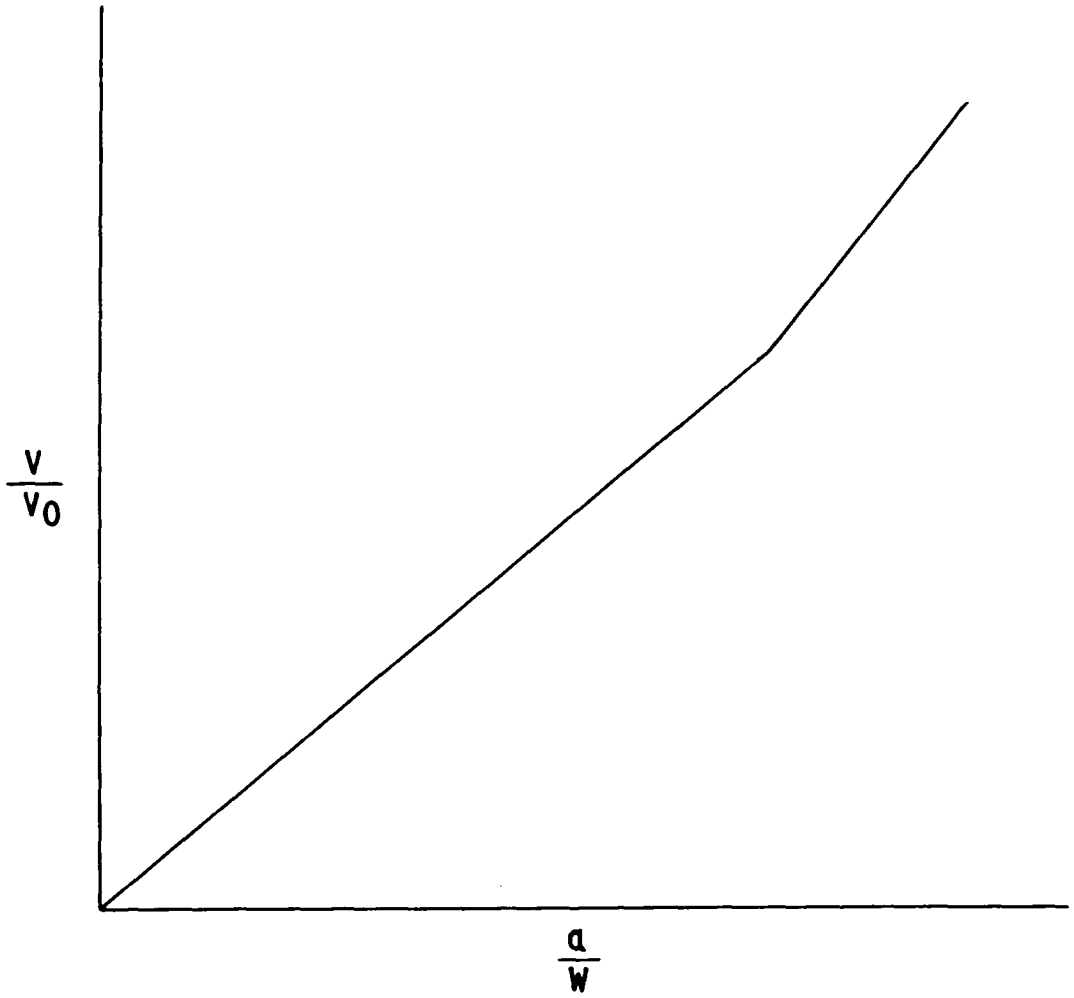

FIG. 14. P. D. / $\frac{a}{W}$ CURVE

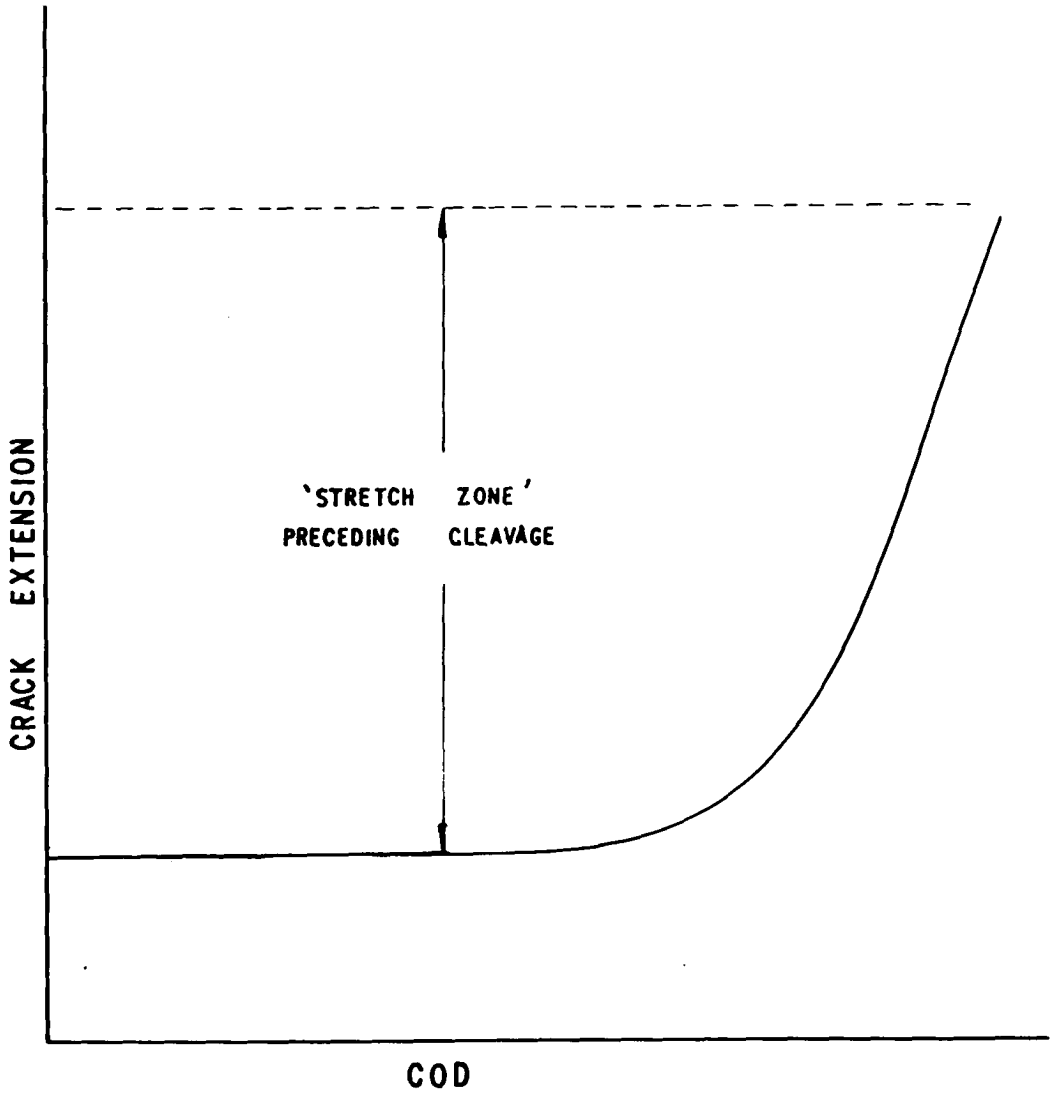

FIG. 15 DUCTILE CLEAVAGE BEHAVIOUR.

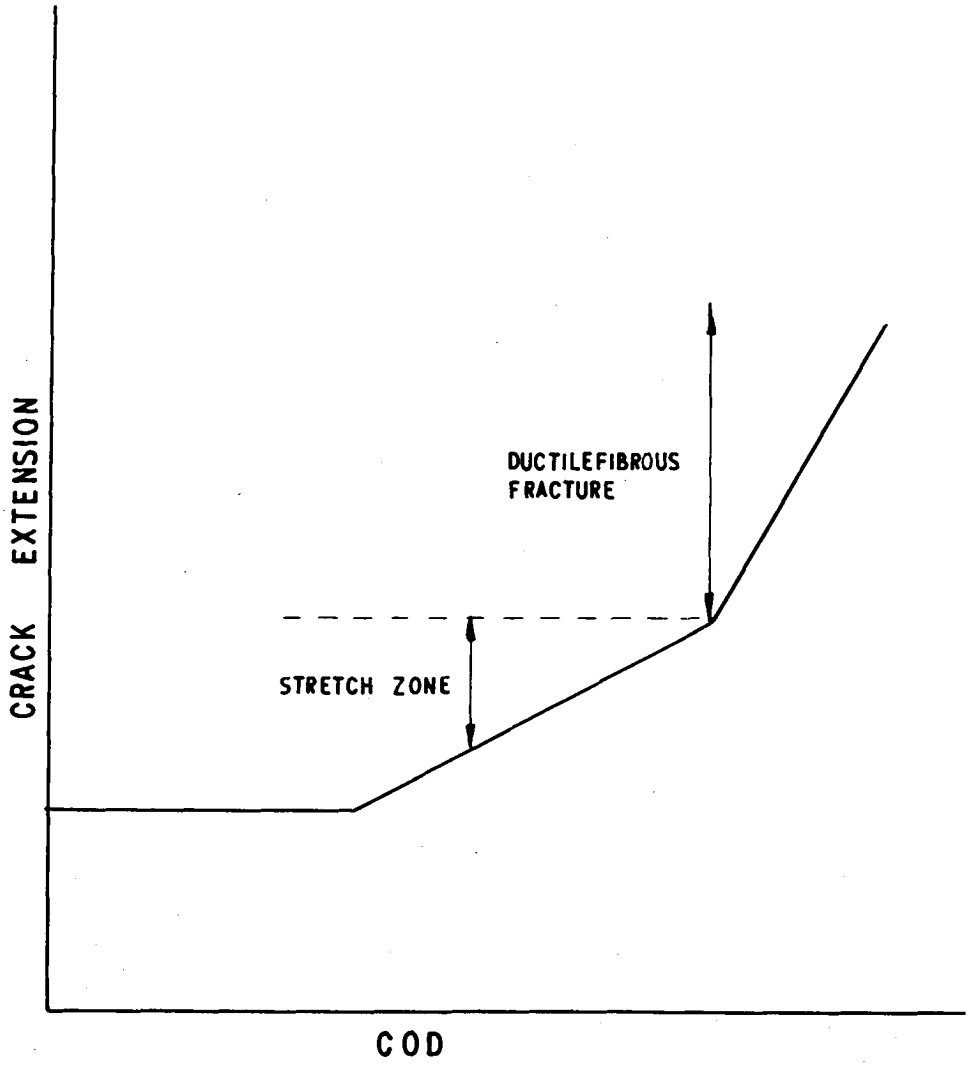

FIG. 16 DUCTILE FIBROUS BEHAVIOUR.

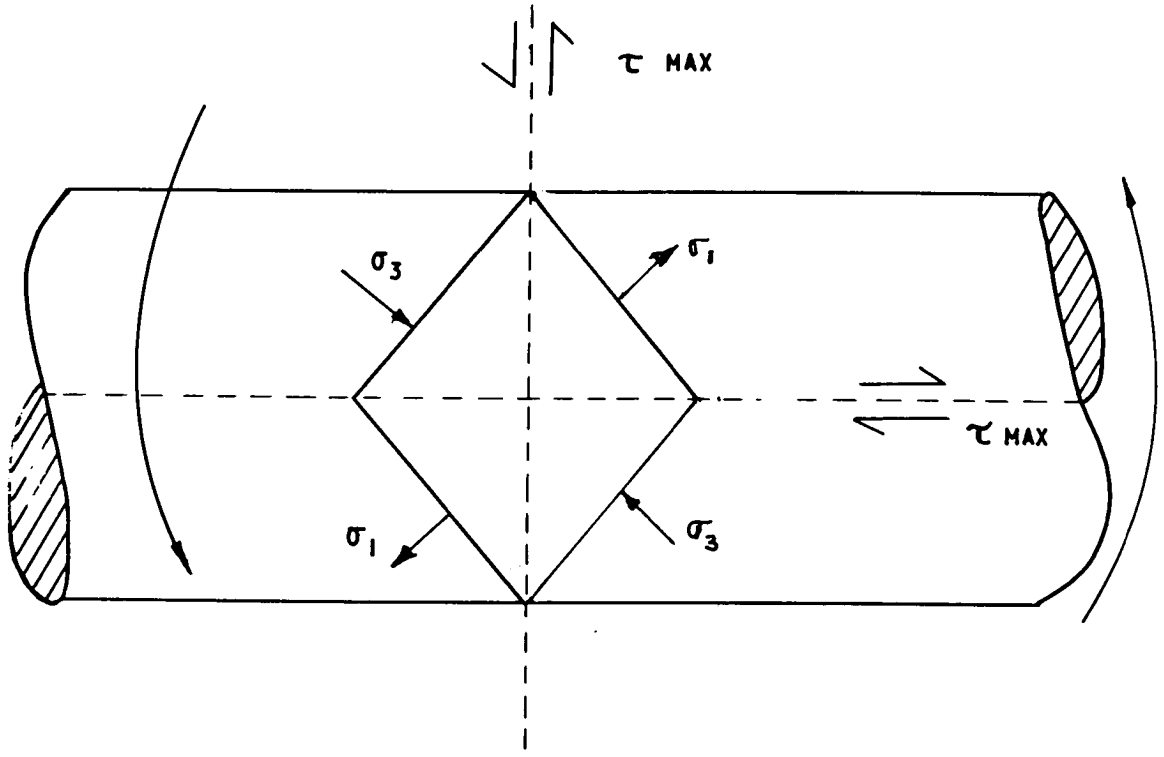

FIG. 17 TORSIONAL STRESS STATE IN A HELICAL SPRING.

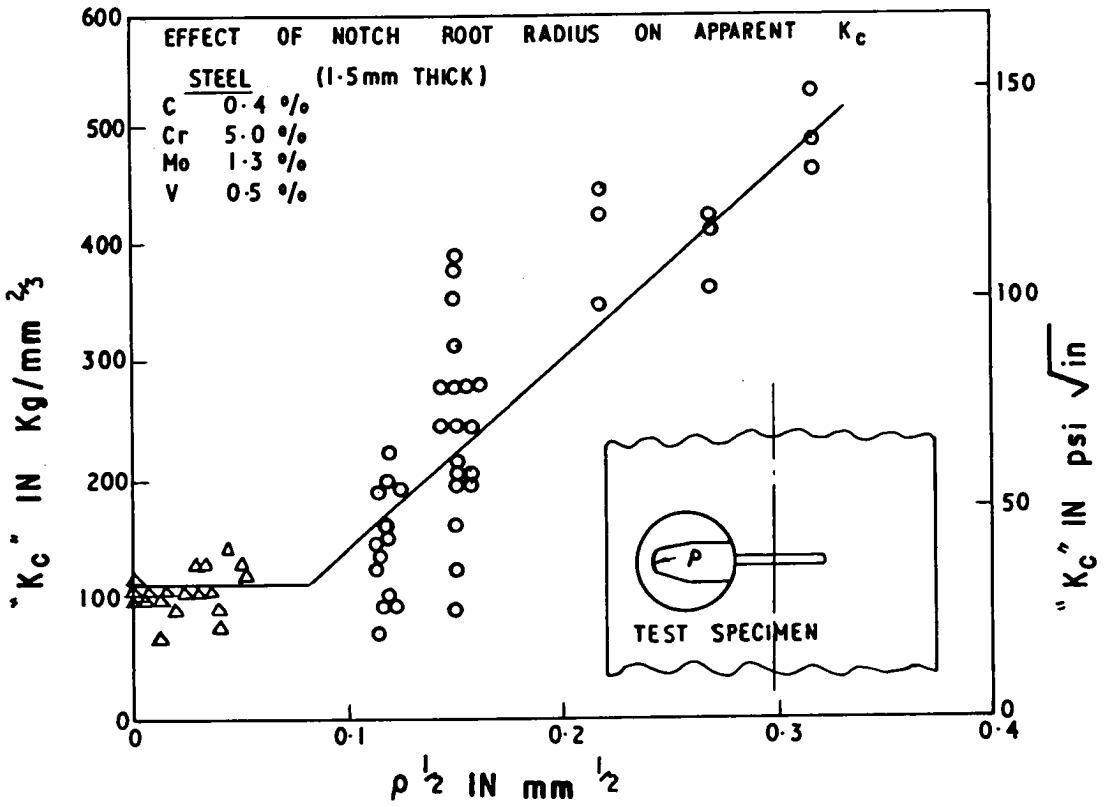

FIG. 18 VARIATION OF FRACTURE TOUGHNESS WITH NOTCH ROOT RADIUS. (FROM REF. 4.)

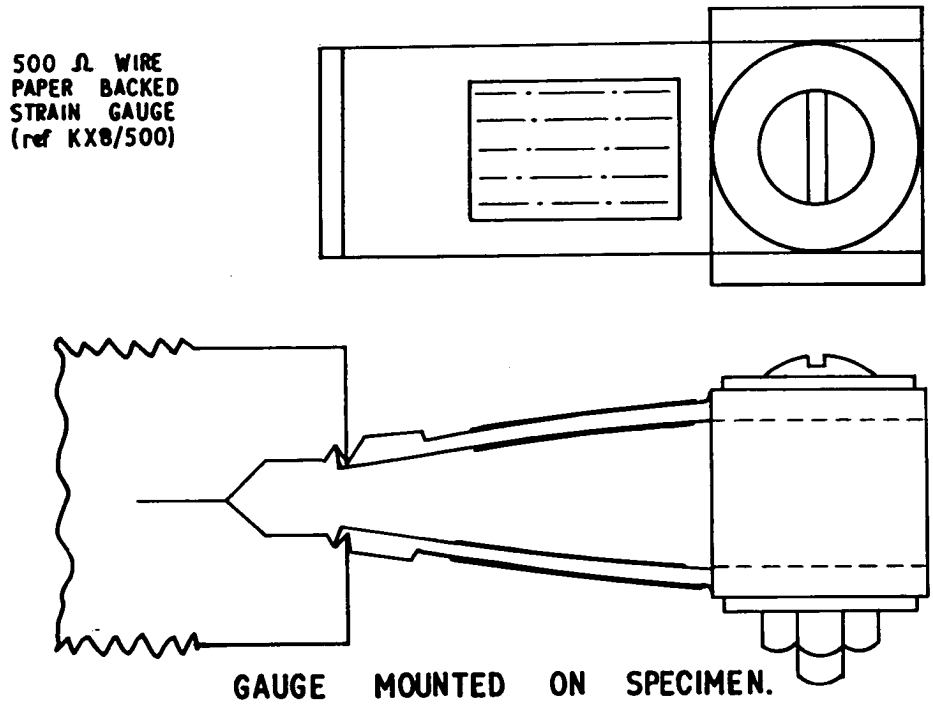

FIG. 19 DESIGN OF CLIP GAUGE FOR TOUGHNESS TESTING. (FROM REF. 4.)